INTERNATIONAL JOURNAL FOR NUMERICAL METHODS IN FLUIDS, VOL. 11, 571–585 (1990)

ON THE QUALITY OF VISCOELASTIC FLOW SOLUTIONS: AN ADAPTIVE REFINEMENT STUDY OF A NEWTONIAN AND A MAXWELL FLUID

REKHA R. RAO AND BRUCE A. FINLAYSON

Department of Chemical Engineering, The University of Washington, Seattle, Washington 98195, U.S.A.

SUMMARY

Little adaptive finite element work has been done in the area of viscoelastic flow in complex geometries. In this paper an adaptive finite element mesh refinement study is carried out on a Newtonian fluid and a Maxwell fluid in an axisymmetric 4:1 contraction. The error indicator used for the refinement is the local norm of the residual in an element. For the Newtonian fluid, steady improvement with refinement is seen, though this is not the case for the Maxwell fluid, which never achieves a solution of good quality.

KEY WORDS Adaptive finite element methods Viscoelastic fluids Newtonian fluids

INTRODUCTION

In recent years, as numerical methods have become more widely used for solving most types of differential equations, interest has grown in methods which can be made to conform or 'adapt' to the problem of interest. Adaptive strategies can be applied to almost any numerical method (finite difference, finite element, collocation or even the choice of integration packages) and generally involve using an initial solution obtained to re-solve the problem in order to achieve a better solution. The advantages of adaptation are obvious: a better solution is obtained for the same computing cost and an inexperienced user can now obtain results similar to those of an experienced user.

Applying this methodology to the finite element method involves calculating the approximate solution to the set of differential equations and boundary conditions of interest on an initial coarse mesh and from this calculating some type of *a posteriori* error indicator. The interpolation of the exact solution is then improved by one of several adaptive techniques, which include adaptive remeshing, adaptive node movement and adaptive refinement. Two types of adaptive refinement exist: *p*-enrichment involves raising the order of the polynomials used to interpolate the solution while *h*-enrichment involves decreasing the element size. A more detailed discussion of these adaptation schemes is included below, along with a general discussion of error indicators and estimators. The final section of the introduction discusses the work which has already been carried out on the application of adaptive finite element analysis to viscoelastic (VE) flow problems.

Remeshing

Application of adaptive remeshing involves producing a new mesh at each iteration or time step based on the error indicators from the previous solution. This technique is not that widely used, since producing a new mesh at every stage of the calculation and interpolating the previous

0271–2091/90/130571–15$07.50

Received December 1988
Revised November 1989

solution onto the new mesh are very expensive processes. However, the convergence properties of this method are good, since the performance of the finite element method depends greatly on the choice of mesh.

This method is particularly applicable to problems in one dimension[1] where grid regeneration is relatively cheap, problems containing one-dimensional features such as shocks, and problems with wavefronts where the position of greatest change in the solution moves with time. Almost any grid generation program, for either triangular or quadrilateral elements, which contains an element or node density function can be converted into an adaptive remeshing scheme: all that needs to be done is to relate the error indicator to the density function.[2] The error indicator is calculated on an initial non-optimal mesh (a uniform grid is often utilized) and a new mesh is produced based on the new density function. The previous solution is then interpolated onto the new mesh. Explicit node or element density functions are most often found for mapping-based mesh generation programs.

For unstructured grid generation programs which contain no explicit density function, other techniques can be used. Frey[3] calculates a solution on an initial coarse triangular mesh, adds a node to the centre of all elements where the error indicators are high, and then retriangulates on the basis of this new nodal structure. Peraire *et al.*[4] calculate an element size as each element is formed and therefore do not need a global density function. Much success has been demonstrated when this method was used in conjunction with *h*- or *p*-refinement.[5] This method has also been used together with *r*-type adaptation for problems with moving boundaries.[6]

Mesh movement

Mesh movement or *r*-type adaptation is the method which has been used the longest of all adaptive techniques, beginning in the early 1970s with the work of Oliveira.[7] This method is severely limited by the choice of initial mesh. Node relocation will probably improve the quality of the solution, but optimization of the mesh is easier to achieve with one of the other adaptive strategies which add degrees of freedom. The essence of this method consists of moving nodes while maintaining the same element connectivity in order to satisfy certain criteria: either to equidistribute the value of the error indicator or to adapt according to the domain for moving boundary problems. The former is generally achieved using a weighted smoothing related to the error criteria to move the nodes in the necessary direction to smooth the error: conditions to ensure near-orthogonality can also be included. Other constraints must be applied to insure that there is no mesh tangling or node crossing. For cases with singularities the nodes tend to pile up at the singularity (where the error is usually greatest); this must be prevented as well. Moving boundary problems use the insights into the physics of the problem provided by the solution to reposition the nodes.

One advantage of node relocation is that the number of degrees of freedom remains unchanged while the solution is improved. This method is also less expensive than remeshing, since all that need to be recalculated are the new nodal positions. This method is particularly suited to time-dependent problems, where the domain of interest is changing, and shape optimization.[8] It is also useful for problems where the position of steepness of the solution changes with time, such as problems with shocks or wavefronts.[9] For these types of problems it is not necessary to increase the number of degrees of freedom used, but it is important to have good resolution of the solution in regions of steep gradients. For a review of node redistribution see Eiseman.[10]

Mesh refinement

Element refinement consists of increasing the number of degrees of freedom used in regions where the resolution of the solution is inadequate as demonstrated by the value of the error

indicators. Two methods are commonly used in order to achieve this end: *h*-enrichment involves physically refining elements, while *p*-enrichment involves raising the order of the finite element trial function used to interpolate the solution without changing the physical mesh. The development of *h*-version refinement has been credited to Babuška,[2] while *p*-version refinement has been associated with Szabo and Mehta.[11] Both these methods are dependent on the choice of initial mesh and it has been demonstrated by Babuška and Szabo[12] that judicious use of the two methods together produces optimum convergence rates. This has been termed a 'pony express' policy.[13] *h*-Refinement methods tend to be easier to apply since they can be added to existing finite element codes with only minor modifications and for this reason seem to have been more widely used in the past than their *p*-type counterparts, though *p*-refinement has demonstrated superior convergence for a wide number of problems.[12,14,15]

Finite elements are usually at least C^0-continuous, meaning that the solution is continuous across element boundaries (C^1-continuity would mean that both the solution and the first derivative of the solution are continuous across element boundaries). This continuity is ensured by the fact that all the nodes on element sides are shared by their side neighbours. Nodes on element boundaries which are not shared by their side neighbours will be termed 'non-conforming nodes' in the discussion below.

h-Enrichment

This method, involving the subdivision of elements, can be applied with great flexibility to either triangular or quadrilateral elements, and a wide number of different refinement techniques can be applied to either element type.

The refinement of triangular elements can generally be accomplished without creating any non-conforming nodes, because of the unstructured nature of triangular meshes. If a new node is created from an element side, then the node must also be used by its neighbour on that side. In other words, this element must be refined too, though the refinement need not be as severe. For instance, if we quadrasect an element flagged for refinement, we need only bisect its neighbour containing the non-conforming node. Actual physical refinement can be carried out in a number of ways: some like to bisect the longest side of an element to create two elements out of a parent element,[16] while others choose to maintain aspect ratios by creating four new elements from a parent element by bisecting each side and having an embedded centre element with vertices at the bisections.[17] The former technique can produce elements with degraded aspect ratios unless some type of smoothing is used, at an added cost, while the latter technique can produce vast differentials in element size which can have associated problems.[4] It is also possible to refine a triangular element by subdividing it into three quadrilateral elements.[18]

For structured quadrilateral meshes, refinement is often more difficult. If one quadrilateral parent element is subdivided into four elements based on side bisection, non-conforming nodes are produced on each side. Several methods have been used to deal with these nodes. Most commonly, the nodes are left as non-conforming and constraints are used to ensure that the solution will be continuous. These constraints can be handled at the elemental level *via* static condensation or globally using Lagrange multipliers or static condensation.[19] However, constraint equations do add to the computing costs of the solution and the complexity of the program.

For this reason it is often advantageous to refine elements containing non-conforming nodes and eliminate the need for constrained nodes. This will increase not only the degrees of freedom used and the computing costs, but also, sometimes, the accuracy of the solution. Kikuchi[2] uses triangular elements in conjunction with quadrilateral ones to eliminate non-conforming nodes: if the elements next to the subdivided parent element contain non-conforming nodes, the neighbour is split into three triangular elements all sharing the now conforming node. No new non-

conforming nodes are produced in the second subdivision. Marchal *et al.*[20] have compared additional refinement with triangles and constraining non-conforming nodes, and report that constraints worked better for their problems.

Criteria for adaptation

In all of the references discussed above, some type of error indicator was used in order to guide the finite element program to adapt the mesh correctly. This can also be termed a criterion for adaptation and it always has a local character. An error indicator is usually a projection of where more degrees of freedom should be placed in order to reduce the error by the greatest amount. An optimal mesh will have equidistributed errors. This can be accomplished by extrapolating the change in error from the previous solution to the present one,[21] or more complex methods can be used to estimate the change in error by relating the stiffness matrices and right-hand side of the previous and future solutions.[22] A vast number of different indicators have been used successfully, some of which take into account the error in all degrees of freedom and others which only determine the error for one scalar variable. Early workers in the field, such as Oliveira[7] and Turke and Mcneice[23] use an error indicator related to the variational principle of the problems they are solving.[24] Since they are minimizing the scalar functional F, they choose as a natural error indicator the change in F with nodal location, $\mathrm{d}F/\mathrm{d}x$. In the limit as F becomes a true minimum, $\mathrm{d}F/\mathrm{d}x$ will go to zero. Therefore the magnitude of this quantity seems an apt criterion for adaptation: if $\mathrm{d}F/\mathrm{d}x$ is large, the mesh will not be good.

For problems in linear elasticity the errors in the strain energy and the potential energy have been very popular error indicators,[12,22] since minimization of these quantities implies an optimum mesh in a similar manner to the above since they are related to the functionals being minimized. For compressible flow problems the smoothness of the density can be used as the indicator[4,25] and for incompressible flow other gradients of scalars can be used such as temperature or concentration.[26] Norms of velocity or pressure gradients may be used as well. The residual of the discretized differential equations has also been used,[27] as has the energy norm of the error. These quantities have been shown to be related for various problems.[21,28,29]

Criteria for ending calculations

Much work has been done in recent times in the area of obtaining good *a posteriori* error estimates for the finite element method. For problems which have been well studied, such as linear elliptic problems[30] and linear parabolic problems,[31,32] there exist advanced methods of estimating the error. For non-linear problems, less work has been done and good *a posteriori* error estimates are not yet available.[24] However, workers such as Zienkiewicz and Babuška have been implying that good non-linear error estimators are on their way.[21,22]

Error estimators can be either local or global: a local error estimate can be used as an error indicator and transformed into a global error by summing over all the elements. The reliability of the error estimator can be demonstrated using an effectivity index

$$\theta = \frac{\varepsilon}{\|e\|}, \tag{1}$$

where ε is the error estimate and e is the true error. We can have either upper or lower estimators. The estimator will be asymptotically correct if

$$\lim_{\theta \to 1} \|e\| \to 0. \tag{2}$$

In fact, Babuška and Rheinboldt[21] have shown that for some problems the error estimator only gives reliable estimates in this limit. Before this the mesh is non-optimal: its error is not equilibrated and the error estimator is not efficient.

For problems where no good error estimate is available, the amount of computer time used or memory requirements are good criteria for stopping calculations. The quality of the solution, as judged by the engineer, can be another stopping criterion. Also, if the error indicators have stopped changing, the calculation can be discontinued. In these cases the user does know when to discontinue the adaptive cycle, but he has not gotten as much information about the solution as he would have if an appropriate error estimator had been available.

Application of adaptive finite element analysis to viscoelastic flow problems

Little adaptive work has been done in the field of non-Newtonian fluid mechanics since most workers have been concerned with the 'high-Weissenberg-number problem',[20,33] which describes the convergence failure of the numerical scheme as the amount of elasticity in the fluid is increased. Marchal *et al.*[20] study the flow of a Maxwell fluid around a sphere and use the positive definiteness of the finger strain tensor as their criterion for refinement. The mesh consists of quadrilateral elements and they refine in the manner discussed above, using constrained nodes. These workers were trying to increase the critical Weissenberg number with this method: they were unsuccessful. They did demonstrate an improvement in the solution away from the stagnation point with refinement. However, near the stagnation point the solution seemed to deteriorate upon refinement.

Brown *et al.*[33] study the flow of a Maxwell fluid through an abrupt 4:1 contraction. They refine in the same way as Marchal *et al.*,[20] but since they have no error indicator, they manually refine elements. They demonstrate that the critical Weissenberg number decreases with adaptive refinement and that convergence for any Weissenberg number becomes more difficult as the refinement near the singularity is increased.

Pursuing knowledge in the field of adaptive finite element analysis is important because it can become a very powerful technique for efficient problem solving for viscoelastic flow once the 'high-Weissenberg-number problem' has been alleviated. In this spirit an investigation is made into the differences between adaptive *h*-enrichment for a Newtonian fluid and a viscoelastic fluid, both in an abrupt cylindrical 4:1 contraction.

EQUATIONS AND METHOD

Equations

The dimensionless equations describing the steady flow of an upper-convected Maxwell fluid are the Cauchy momentum equation

$$Re\,\mathbf{u}\cdot\nabla\mathbf{u} = -\nabla p - \nabla\cdot\boldsymbol{\tau}, \tag{3}$$

the continuity equation

$$\nabla\cdot\mathbf{u} = 0 \tag{4}$$

and the constitutive equation

$$\boldsymbol{\tau} + We\,\boldsymbol{\tau}_{(1)} = -\dot{\gamma}, \tag{5}$$

where

$$\dot{\gamma} = \nabla \mathbf{u} + \nabla \mathbf{u}^{\mathrm{T}}, \tag{6}$$

$$\dot{\gamma} = [\tfrac{1}{2}\dot{\gamma} : \dot{\gamma}]^{1/2}, \tag{7}$$

$$\tau_{(1)} = \mathbf{u} \cdot \nabla \tau - \nabla \mathbf{u}^{\mathrm{T}} \cdot \tau - \tau \cdot \nabla \mathbf{u}. \tag{8}$$

The dimensionless parameters are

$$Re = \frac{\rho \langle u \rangle R}{\mu} \quad \text{and} \quad We = \frac{\lambda \langle u \rangle}{R}, \tag{9}$$

where ρ is the density, $\langle u \rangle$ is the average velocity upstream, R is the downstream radius, λ is the time constant, Re is a Reynolds number and We is a Weissenberg number. The Weissenberg number is a dimensionless elastic time constant. Another dimensionless parameter of interest is the recoverable shear (S_{R}), which is defined as

$$S_{\mathrm{R}} = We \dot{\gamma}_{\mathrm{W}}, \tag{10}$$

where $\dot{\gamma}_{\mathrm{W}}$ is evaluated at the downstream wall at the exit. The boundary conditions used for the cylindrical 4:1 contraction problem are fully developed flow upstream and downstream from the contraction, symmetry about the centreline and no slip at the solid boundary. Fully developed values of the stress fields are also specified at the inlet:

$$\tau_{rr} = 0, \qquad \tau_{rz} = -\dot{\gamma}, \qquad \tau_{zz} = 2We\dot{\gamma}^2, \qquad \mathrm{tr}\,\tau = \tau_{zz}. \tag{11}$$

The pressure is specified at one point since the pressure field is indeterminate to a constant; here the downstream wall is used. All boundary conditions are shown in Figure 1.

Galerkin finite element method

The above equations and boundary conditions are discretized and solved with the Galerkin finite element method. The velocity fields are interpolated with biquadratic trial functions,

$$u = \sum_{i=1}^{n} u_i N_i(r, z), \tag{12}$$

$$v = \sum_{i=1}^{n} v_i N_i(r, z), \tag{13}$$

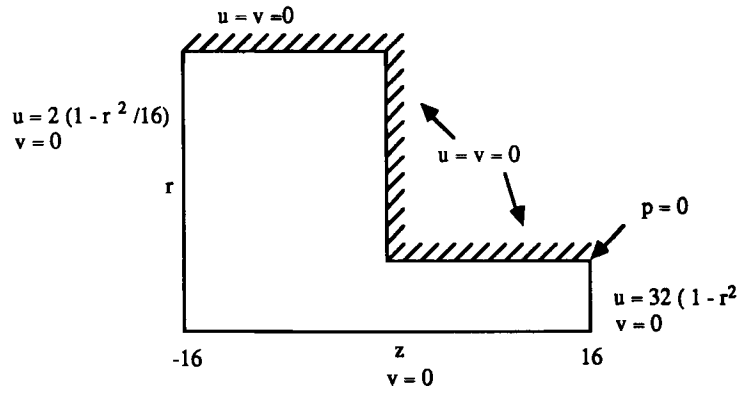

Figure 1. Boundary conditions for an axisymmetric 4:1 contraction

while the pressure and stress fields are represented by bilinear trial functions,

$$p = \sum_{i=1}^{n} p_i N_i'(r, z), \tag{14}$$

$$\tau_q = \sum_{i=1}^{n} \tau_{qi} N_i'(r, z), \tag{15}$$

where the subscript q denotes either the rr-, zz-, or rz-component of the stress tensor or the trace. The discretization of the domain is carried out with Lagrangian triangular elements.

The constitutive equation (5) is first substituted into the momentum equation (3) to obtain

$$Re\,\mathbf{u}\cdot\nabla\mathbf{u} = -\nabla p - \nabla\cdot\dot{\gamma} + We\,\nabla\cdot\tau_{(1)}. \tag{16}$$

Next, the trial functions are substituted into equations (16), (4) and (5) in place of the continuous solution. The equations are then weighted with the shape functions themselves, and the divergence of the stress and pressure in equation (16) are integrated by parts. The Galerkin method produces a set of non-linear algebraic equations which are then linearized and solved with a Newton–Raphson method.

The residual

The local L_2-norm of the residual of the discretized differential equations is used as the basis of the adaptive refinement procedure. Consider first a linear problem written in a generalized form

$$\mathbf{L}\mathbf{u} = \mathbf{f}, \tag{17}$$

where $\mathbf{L}$ is the differential operator, $\mathbf{u}$ is the exact solution vector and $\mathbf{f}$ is the right-hand side of the equations. If the approximate solution is substituted for the continuous solution, an expression for the residual is obtained.

$$\mathbf{r} = \mathbf{L}\mathbf{u}_h - \mathbf{f}, \tag{18}$$

where $\mathbf{r}$ denotes the residual and $\mathbf{u}_h$ is the approximate solution vector. Combining equations (17) and (18) gives an expression relating the residual and the error:

$$\mathbf{r} = \mathbf{L}(\mathbf{u}_h - \mathbf{u}) = \mathbf{L}(\mathbf{e}). \tag{19}$$

If $\mathbf{u}_h$ were the exact solution, then the the residual would be zero. Thus the residual gives some measure as to how well the differential equations are satisfied. In some cases, when an appropriate Green's function is available and bounded, or a minimum or maximum variational principle is available, equation (19) can be inverted and the error can be related directly to the residual. Formally this is expressed as

$$\mathbf{e} = \mathbf{L}^{-1}\mathbf{r}, \tag{20}$$

$$\|\mathbf{e}\| \leqslant \|\mathbf{L}^{-1}\mathbf{r}\| \leqslant \|\mathbf{L}^{-1}\|\,\|\mathbf{r}\|. \tag{21}$$

For non-linear partial differential equations such bounds are rarely available, though the use of the residual to assess the quality of the solution is still a possible option. The use of the residual as an error indicator is largely empirical for the non-linear differential equations and complex boundary conditions governing viscoelastic flow. However, we have demonstrated previously that the behaviour of the residual is related to the quality of the solution.[34]

Once a solution is found, the residual of each differential equation is calculated on an element. We define an element residual $|\mathbf{r}_e|$ as

$$|\mathbf{r}_e| = \left(\sum_{i=1}^{7} \int_{\Omega_e} r_{ei}^2 \, d\Omega \right)^{1/2}, \tag{22}$$

where r_{ei} denotes the residual of one of the seven equations in an element (two momentum, three stress, continuity and trace stress) and $d\Omega$ denotes an integral over the entire area. This form of the norm is chosen since there are seven residuals of interest which all need representation; however, the residuals of the momentum equations are generally the largest and thus dominate equation (22). We also calculate an average residual over all elements,

$$\text{average residual} = \frac{1}{\text{NE}} \sum_{e=1}^{\text{NE}} |r_e|, \tag{23}$$

and a maximum over all elements,

$$\text{maximum residual} = \max_{1 \leq e \leq \text{NE}} |r_e|. \tag{24}$$

These quantities are used in the actual adaptation. For each solution, however, we also calculate the norm of the residual for each equation i:

$$\|r_i\| = \left(\sum_{e=1}^{\text{NE}} \int_{\Omega_e} r_{ei}^2 \, d\Omega \right)^{1/2}. \tag{25}$$

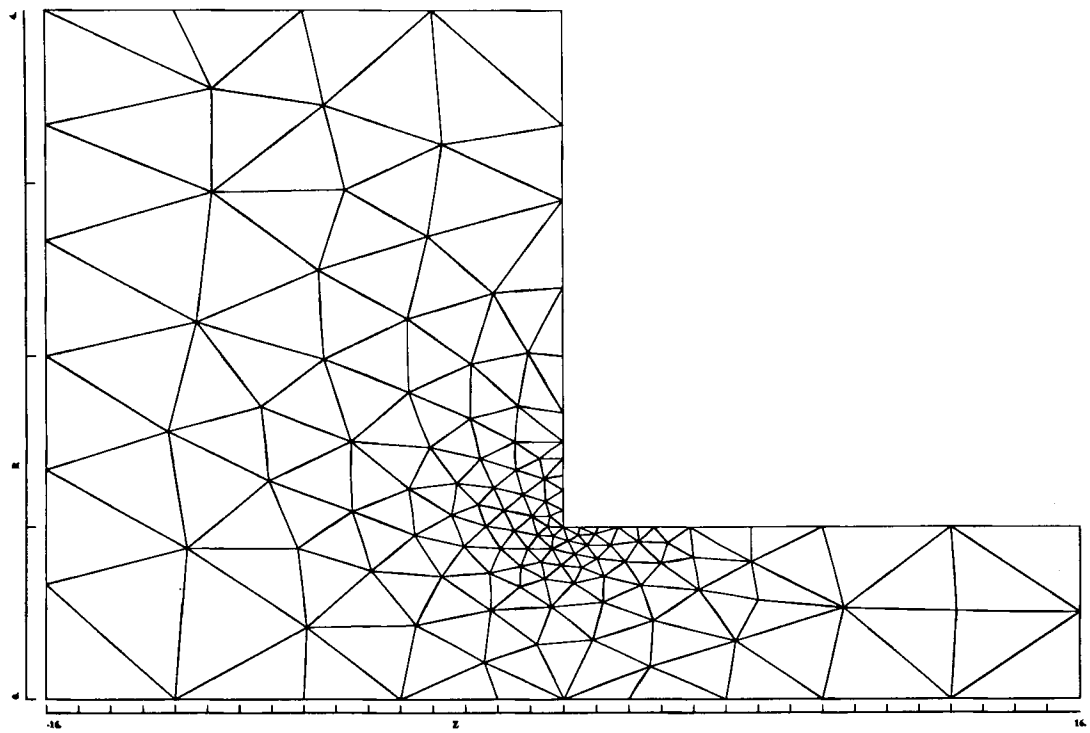

Figure 2. Initial axisymmetric 4:1 contraction mesh for the adaptive refinement study

Adaptive refinement

The adaptive analysis begins with calculation of the solution on the initial coarse mesh which is given in Figure 2. Once a convergent solution is achieved, the norm of the residual is calculated in each element. The average value of the norm over all elements is then calculated. Elements having residuals greater than twice the average are flagged for refinement. The flagged elements are then bisected along their longest side to form two new triangular elements from one parent element. As the mesh is adapted, the previous solution is interpolated onto any new nodes formed, providing a good starting guess for the Newton–Raphson iteration of the next stage of adaptation.

After all the necessary elements have been refined, Gaussian smoothing is applied, which places each node at the centroid of a polygon formed by its neighbours. This tends to form elements which are shaped more closely to equilateral triangles. Finally, an element reordering scheme is applied in order to minimize the element front width[35] and solve the problem as efficiently as possible.

The adaptation process is continued three times in turn, at which point it is terminated owing to excessive computer time. It is interesting to note that once a larger computer was available for calculations another refinement stage was attempted. Four refinement stages were achievable for the Newtonian fluid, while the Maxwell fluid did not have a convergent solution after four refinements. The solution to the Newtonian problem converged in one iteration, while the Maxwell fluid solution took four iterations to converge. The time it takes to physically refine the mesh is less than one-tenth of the time for one iteration.

Contour plotting

Contour plots are produced from an existing finite element mesh of triangles by subdividing the triangular element into six smaller triangles and then drawing straight-line contours across these subdivisions. The values of the contours plotted are chosen on the basis of the field values on the initial mesh. First, the maximum and minimum values of the field being plotted are determined on the initial mesh. Next, 10 evenly spaced contour values are calculated between the maximum and minimum values. These contour values are also used for the contour plots of the more refined meshes for ease of comparison.

RESULTS

An adaptive refinement study was carried out for both a Newtonian and a non-Newtonian fluid in Stokes flow ($Re=0$) in a cylindrical 4:1 contraction. The Maxwell model constitutive relation given in equation (5), with an S_R of 1·28, was used to represent the viscoelastic behaviour of the fluid. Figure 3 demonstrates how the mesh changes as a function of refinement for the Newtonian fluid. Figure 4 contains similar representations for the Maxwell fluid. For both fluids, most of the refinement occurs near the re-entrant corner. This is as we would expect since there is a singularity in the solution there. One difference between the fluids as we refine the meshes is that the mesh for the Newtonian fluid becomes more refined at the centreline near the plane of contraction than the viscoelastic fluid's mesh. For the viscoelastic fluid the singularity at the re-entrant corner dominates the refinement process.

Let us first examine how the solution changes with adaptation for the Newtonian fluid. Figure 5 contains contour plots of the *rr*-stress for the initial and final adaptive refinement stages; these are plotted with the same contour values for ease of comparison. The *rr*-stress on the initial mesh is plagued by large jagged contours which will be referred to as oscillations. The solution improves at each refinement stage. On the final refinement the solution looks quite good: most of the

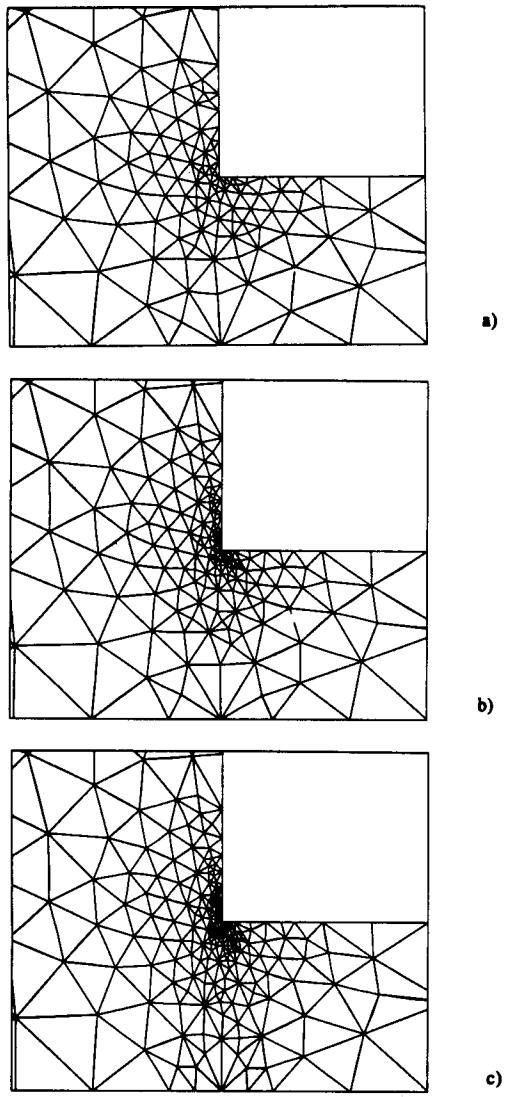

Figure 3. Corner detail of the adaptive meshes as a function of refinement for the Newtonian fluid ($0 \leqslant r \leqslant 2$, $-8 \leqslant z \leqslant 8$): (a) first refinement; (b) second refinement; (c) third refinement

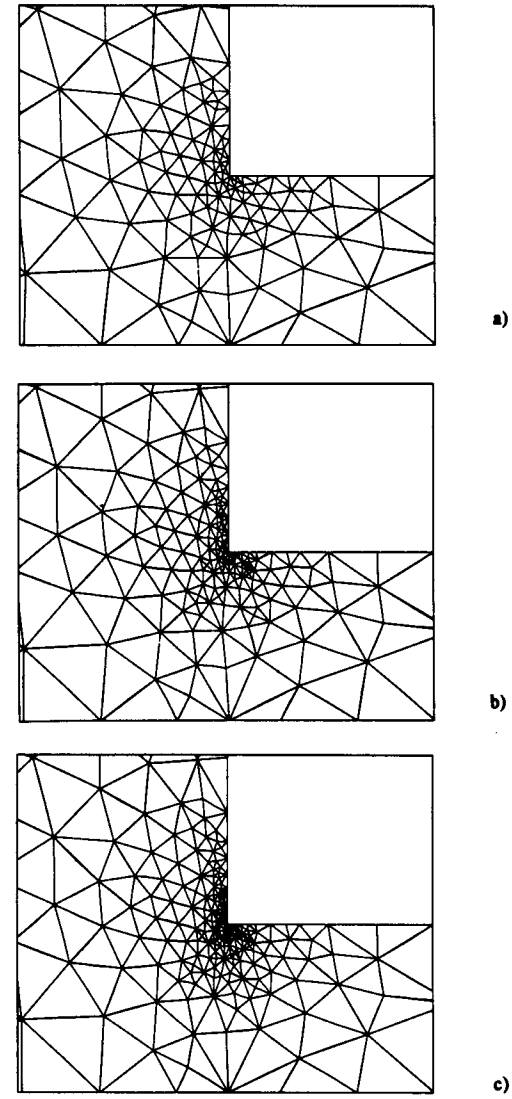

Figure 4. Corner detail of the adaptive meshes as a function of refinement for the Maxwell fluid ($0 \leqslant r \leqslant 2$, $-8 \leqslant z \leqslant 8$): (a) first refinement; (b) second refinement; (c) third refinement

oscillations are gone and the distance between contours has decreased, implying better resolution of the stress near the singularity.

Figure 6 contains contour plots of the *rz*-stress for the Newtonian fluid as a function of refinement. These plots also demonstrate improvement upon refinement, though not as dramatically as the plots of the *rr*-stress. The quality of the solution increases as we refine the mesh and more details of the solution are represented. The solution generally becomes smoother as well. Are the results we obtain for the Maxwell fluid similar to those obtained for the Newtonian fluid?

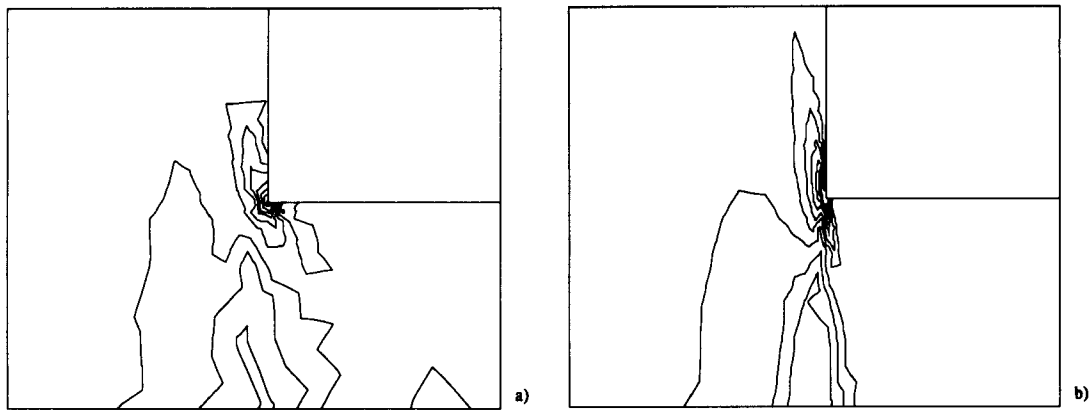

Figure 5. Corner detail of the *rr*-stress for a Newtonian fluid on the initial and most refined mesh ($0 \leqslant r \leqslant 2$, $-8 \leqslant z \leqslant 8$) (contour values: −37·3, −31·8, −26·3, −20·9, −15·4, −10·0, −4·4, 1·1, 6·6, 12·1): (a) initial mesh; (b) third refinement

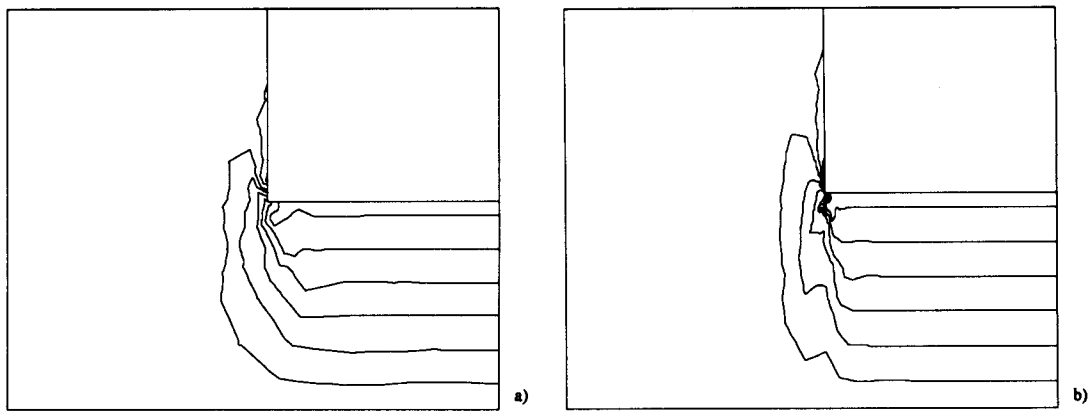

Figure 6. Corner detail of the *rz*-stress for a Newtonian fluid on the initial and most refined mesh ($0 \leqslant r \leqslant 2$, $-8 \leqslant z \leqslant 8$) (contour values: −15·0, −6·0, 3·0, 12·0, 21·0, 30·1, 39·1, 48·1, 57·1, 66·1): (a) initial mesh; (b) third refinement

Figure 7 contains plots of the *rr*-stress on the initial and final mesh for the Maxwell fluid. The *rr*-stress on the initial mesh contains both large and small oscillations. For the final adaptation stage the solution near the singularity is greatly improved but the unattractive oscillations near the plane of contraction persist. We are seeing an interesting trend: the solution is improving in some regions while in other regions spurious wiggles and erroneous stress islands are appearing.

On viewing Figure 8, which has contour plots of the *rz*-stress for the initial mesh and the final adapted mesh, we can see the same trends as for the *rr*-stress. The solution on the initial mesh lacks detail. This problem is corrected as we refine the mesh, as demonstrated by the fact that the contours are closer together; however, there are still breaks in the curves. For both components of the solution for the Maxwell fluid, the *rr*-stress and the *rz*-stress, the solution improves initially, but then levels off with subsequent adaptation and no further improvement is observed.

We can get more insight into the effects of the singularity on the solution if we look at slices of the solution, for both fluids, taken at the horizontal and vertical planes of the contraction. Figure 9 shows the effect of refinement on the *zz*-stress on the line $r = 1$ from $-5 < z < 5$. The Newtonian

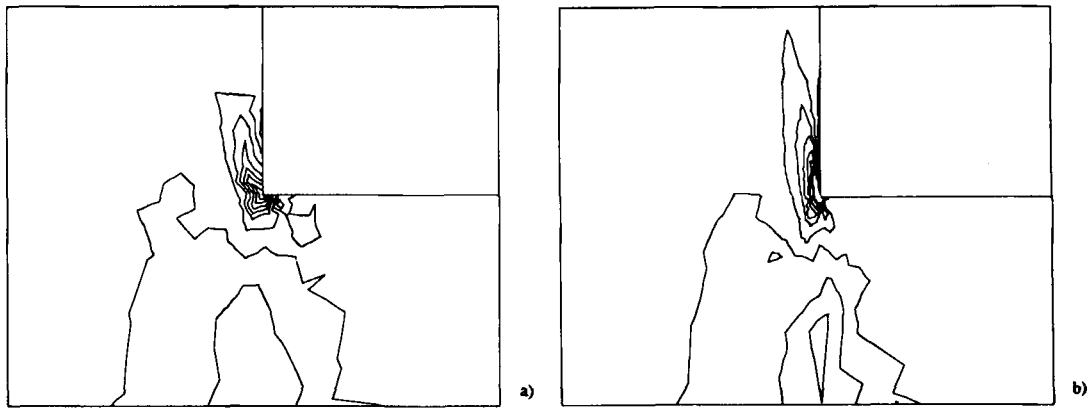

Figure 7. Corner detail of the *rr*-stress for a Maxwell fluid on the initial and most refined mesh ($0 \leqslant r \leqslant 2$, $-8 \leqslant z \leqslant 8$) (contour values: −36·1, −30·9, −25·7, −20·5, −15·2, −10·0, −4·8, 0·4, 5·7, 10·9): (a) initial mesh; (b) third refinement

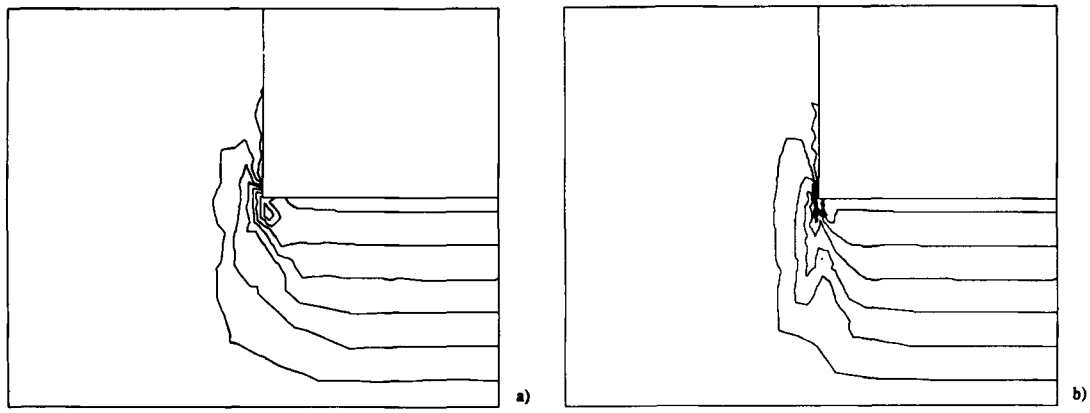

Figure 8. Corner detail of the *rz*-stress for a Maxwell fluid on the initial and most refined mesh ($0 \leqslant r \leqslant 2$, $-8 \leqslant z \leqslant 8$) (contour values: −12·7, −2·4, 8·0, 18·3, 28·7, 39·0, 49·4, 59·7, 70·0, 80·4): (a) initial mesh; (b) third refinement

fluid on the initial mesh has a wide diffuse peak at the singularity and is zero elsewhere, except for a small oscillation. As the mesh is refined, the peak at the singularity becomes larger and sharper and the oscillation becomes smaller. The viscoelastic solution on the initial mesh totally misses the singularity at the re-entrant corner. After three refinement stages a small sharp peak at the singularity is achieved. If we look at the *zz*-stress solution on the line $z = 0$, $0 < r < 2$ (Figure 10), we can see that similar trends are followed; however, the results at this slice are less impressive. The Newtonian solution on the initial mesh is relatively smooth and contains a wide peak at the re-entrant corner. As the mesh is refined, the peak at the corner sharpens but the solution elsewhere becomes less smooth. For the Maxwell fluid on the initial mesh the solution begins with a few large oscillations and a peak slightly below the singularity. After three refinement stages the peak for the singularity has moved closer to the re-entrant corner but now has a snubbed appearance and the oscillations have become more pronounced in the inlet to the small tube. For the Newtonian fluid we have seen a general improvement at each refinement stage. The solution on the final mesh seems to indicate that further refinement is necessary. For the Maxwell fluid there is some

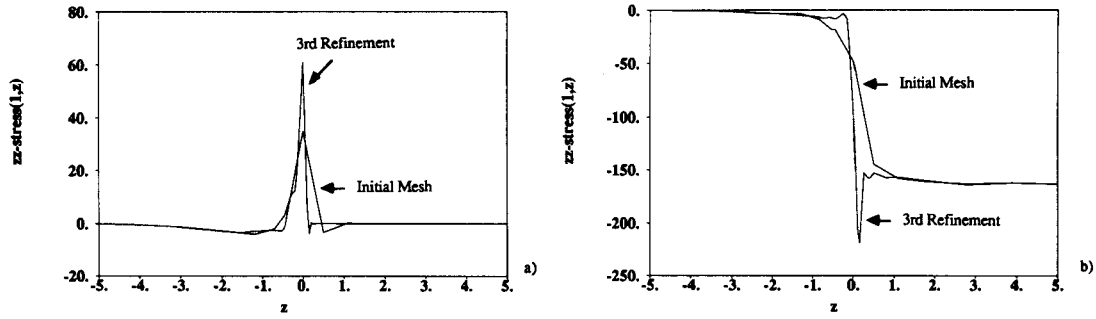

Figure 9. zz-Stress $(1, z)$ $(-5 \leqslant z \leqslant 5)$ at the horizontal plane of the contraction for both fluids as a function of refinement: (a) Newtonian fluid; (b) Maxwell fluid

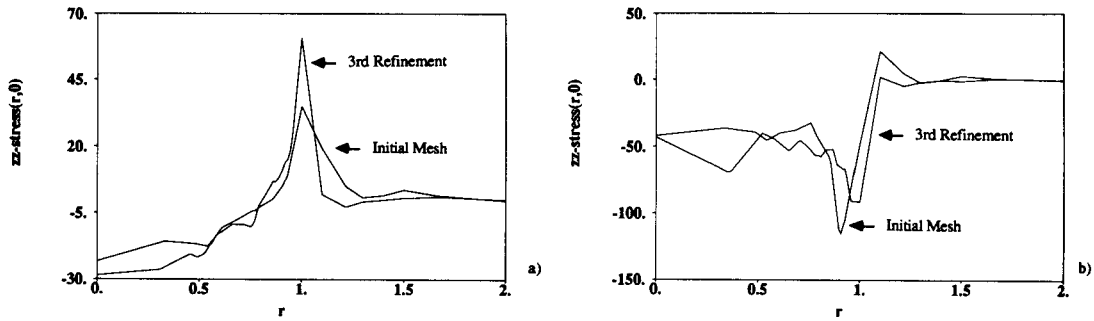

Figure 10. zz-Stress $(r, 0)$ $(0 \leqslant r \leqslant 2)$ at the vertical plane of the contraction for both fluids as a function of refinement: (a) Newtonian fluid; (b) Maxwell fluid

Table I. Refinement information

Fluid[a]	Stage	Unknowns	Nodes	Elements	Average residual[b]	Maximum residual[c]	r-Momentum residual[d]	z-Momentum residual[d]
N	0	1624	482	219	7·4	158·7	119·4	227·6
N	1	1973	589	272	6·8	74·7	136·0	197·0
N	2	2463	739	346	6·7	96·5	160·6	253·1
N	3	3172	956	453	5·0	97·2	180·1	202·2
M	0	1624	482	219	7·9	144·3	174·3	199·8
M	1	1973	589	272	7·0	91·2	184·5	183·0
M	2	2515	354	354	7·3	163·1	280·4	216·0
M	3	3046	435	435	7·1	229·7	331·1	218·8

[a] N, Newtonian; M, Maxwell.
[b] Equation (23).
[c] Equation (24).
[d] Equation (25) for $i = 1, 2$.

improvement with refinement but, in part, the solution actually seems to degrade with refinement. Evidence of this would be the fact that the solution on the fourth refinement of the mesh did not converge.

The trends we see for both fluids are reflected in the error indicator used, the norm of the residual. Table I contains refinement information for both fluids. It gives statistics on the number

of unknowns, nodes and elements for each mesh, as well as the average, maximum and total r- and z-momentum residuals for each equation on every mesh. For the Newtonian fluid the average of the norm of the residual in an element decreases as the mesh is adaptively refined. The maximum norm is also roughly decreasing. For the Maxwell fluid the average residual in an element decreases slightly initially and then levels off, but essentially stays constant. The maximum residual decreases for the first refinement stage and increases for subsequent stages. The norms of the residuals behave similarly; uniform convergence is not yet observed for this difficult problem. The residuals are calculated only at the quadrature points, so that as the mesh is refined there is actually additional detail provided for the calculation of the norm. Thus some of the results from the norm may be due to quadrature error.

An adaptive refinement study was also carried out at a higher value of the recoverable shear, $S_R = 3{\cdot}84$. For this fluid, only one refinement stage was possible, at which time the Newton–Raphson failed to converge. This result agrees with Brown *et al.*[33] An explicitly elliptic form of the momentum equation,[36] which eliminates the destructive coupling between the stress and momentum equations, has been used to extend the S_R-limit. These results will be presented elsewhere.

CONCLUSIONS

Improvement can be seen as the mesh is adapted for the Newtonian fluid and this fact is also reflected in the error indicator which decreases with refinement. Once there is a small amount of elasticity in the fluid, using a Maxwell model, the quality of the solution decays dramatically and we no longer see steady improvement with adaptive refinement. At the final refinement stage a good-quality solution has not yet been achieved. This trend is also reflected in the residual which stays relatively constant with refinement.

REFERENCES

1. M. Bieterman and I. Babuška, 'An adaptive method of lines with error control for parabolic equations of the reaction–diffusion type', *J. Comput. Phys.*, **63**, 33–66 (1986).
2. N. Kikuchi, 'Adaptive grid-design methods for finite element analysis', *Comput. Methods Appl. Mech. Eng.*, **55**, 129–160 (1986).
3. W. H. Frey, 'Selective refinement: a new strategy for automatic node placement in graded triangular meshes', *Int. j. numer. methods eng.*, **24**, 2183–2200 (1987).
4. J. Peraire, M. Vahdati, K. Morgan and O. C. Zienkiewicz, 'Adaptive remeshing for compressible flow computation', *J. Comput. Phys.*, **72**, 449–466 (1987).
5. J. Z. Zhu and O. C. Zienkiewicz, 'Adaptive techniques in the finite element method', *Commun. Appl. Numer. Methods*, **4**, 197–204 (1988).
6. M. R. Albert and K. O'Neill, 'Moving boundary–moving mesh analysis of phase change using finite elements with transfinite mapping', *Int. j. numer. methods eng.*, **23**, 591–607 (1986).
7. E. R. Arantes e Oliveira, 'Optimization of finite element solution', *Proc. Third Conf. on Matrix Methods in Structural Mechanics*, Wright-Patterson Air Force Base, Dayton, OH, 1971.
8. N. Kikuchi, K. Y. Chung, T. Torigaki and J. E. Taylor, 'Adaptive finite element methods for the shape optimization of linearly elastic structures', *Comput. Methods Appl. Mech. Eng.*, **57**, 67–89 (1986).
9. A. R. Diaz, N. Kikuchi and J. E. Taylor, 'A method of grid optimization for the finite element method', *Comput. Methods Appl. Mech. Eng.*, **41**, 29–45 (1983).
10. P. R. Eiseman, 'Grid generation for fluid mechanics', *Ann. Rev. Fluid Mech.*, **17**, 487–522 (1985).
11. B. A. Szabo and A. K. Mehta, 'p-Convergent finite element approximations in fracture mechanics', *Int. j. numer. methods eng.*, **12**, 551–560 (1978).
12. I. Babuška and B. A. Szabo, 'On the rates of convergence of the finite element method', *Int. j. numer. methods eng.*, **18**, 323–341 (1982).
13. R. J. Melosh and S. Uktu, 'Accurate finite element analysis', in H. Kardestuncer (ed.), *Finite Element Handbook*, McGraw-Hill, 1987, pp. 3.401–3.444.
14. B. Guo and I. Babuška, 'The h–p version of the finite element method: Part 1 – The basic approximation results', *Comput. Mech.*, **1**, 21–41 (1986).

15. R. Lohner, 'Finite elements in CFD: what lies ahead?', *Int. j. numer. methods eng.*, **24**, 1741–1756 (1987).
16. M.-C. Rivara, 'A grid generator based on 4-triangles conforming mesh-refinement algorithms', *Int. j. numer. methods eng.*, **24**, 1343–1354 (1987).
17. O. C. Zienkiewicz, Y. C. Liu and G. C. Huang, 'Error estimation and adaptivity in flow formulation for forming problems', *Int. j. numer. methods eng.*, **25**, 23–42 (1988).
18. O. C. Zienkiewicz, Presented at *Int. Conf. of Computational Methods in Flow Analysis*, Okayama, Japan, 1988.
19. M. S. Shephard, 'Automatic mesh generation and adaptive analysis', in H. Kardestuncer (ed.), *Finite Element Handbook*, McGraw-Hill, 1987, pp. 4. 190–4.207.
20. J. M. Marchal, M. J. Crochet and R. Keunings, 'Adaptive refinement for calculating viscoelastic flow problems', in G. F. Carey and J. T. Oden (eds), *Proc. Fifth Symp. of Finite Element and Flow Problems*, Univ. Texas at Austin Press, Austin, TX, 1984, pp. 473–478.
21. I. Babuška and W. C. Rheinboldt, 'A survey of *a posteriori* error estimators and adaptive approaches in the finite element method', in *Proc. China–France Symp. on Finite Element Methods*, Beijing, 1983, Gordon and Breach, New York, pp. 1–65.
22. O. C. Zienkiewicz and J. Z. Zhu, 'A simple error estimator and adaptive procedure for practical engineering analysis', *Int. j. numer. methods eng.*, **24**, 337–357 (1987).
23. D. J. Turke and G. M. Mcneice, 'Guidelines for selecting finite element grids based on an optimization study', *Comput. Struct.*, **4**, 499–520 (1974).
24. N. Kikuchi, Presented at *Int. Conf. of Computational Methods in Flow Analysis*, Okayama, Japan, 1988.
25. R. Lohner, K. Morgan and O. C. Zienkiewicz, 'An adaptive finite element procedure for compressible high speed flow', *Comput. Methods. Appl. Mech. Eng.*, **51**, 441–465 (1985).
26. P. Luchini, 'An adaptive-mesh finite-difference solution method for the Navier–Stokes equations', *J. Comput. Phys.*, **68**, 283–306 (1987).
27. G. F. Carey and D. L. Humphrey, 'Mesh refinement and iterative solution methods for finite element computations', *Int. j. numer. methods eng.*, **17**, 1717–1734 (1981).
28. I. Babuška and W. C. Rheinboldt, 'Adaptive approaches and reliability estimations in finite element analysis', *Comput. Methods Appl. Mech. Eng.*, **17/18**, 519–540 (1979).
29. D. W. Kelly, R. J. Mills, J. A. Reizes and A. D. Miller, '*A posteriori* estimates of the solution error caused by discretization in the finite element, finite difference and boundary element methods', *Int. j. numer. methods eng.*, **24**, 1921–1939 (1987).
30. I. Babuška and W. C. Rheinboldt, '*A posteriori* error estimates for the finite element method', *Int. j. numer. methods eng.*, **12**, 1597–1615 (1978).
31. M. Bieterman and I. Babuška, 'The finite element method for parabolic equations. Part I: *A posteriori* error estimation', *Numer. Math.*, **40**, 339–371 (1982).
32. M. Bieterman and I. Babuška, 'The finite element method for parabolic equations. Part II: *A posteriori* error estimation and adaptive approach', *Numer. Math.*, **40**, 373–406 (1982).
33. R. A. Brown, R. C. Armstrong, A. N. Beris and P.-W. Yeh, 'Galerkin finite element analysis of complex viscoelastic flow', *Comput. Methods. Appl. Mech. Eng.*, **58**, 201–226 (1986).
34. R. R. Rao, T. A. Baer and B. A. Finlayson, 'On the quality of viscoelastic flow solutions', *Proc. Int. Conf. of Computational Methods in Flow Analysis*, Okayama, 1988, pp. 266–273.
35. A. Bykat, 'A note on an element reordering scheme', *Int. j. numer. methods eng.*, **11**, 194–198 (1977).
36. R. C. King, M. R. Apelian, R. C. Armstrong and R. A. Brown, 'Numerically stable finite element techniques for viscoelastic calculations in smooth and singular geometries', *J. Non-Newtonian Fluid Mech.*, **29**, 147–216 (1988).